

Special
Issue

Multifunctional Polyoxometalate Platforms for Supramolecular Light-Driven Hydrogen Evolution**

Salam Maloul,^[a] Matthias van den Borg,^[b] Carolin Müller,^[c, d] Linda Zedler,^[d] Alexander K. Mengele,^[a] Daniel Gaissmaier,^[b, e, f] Timo Jacob,^{*,[b, e, f]} Sven Rau,^{*,[a]} Benjamin Dietzek-Ivanšić,^{*,[c, d]} and Carsten Streb^{*,[a]}

Abstract: Multifunctional supramolecular systems are a central research topic in light-driven solar energy conversion. Here, we report a polyoxometalate (POM)-based supramolecular dyad, where two platinum-complex hydrogen evolution catalysts are covalently anchored to an Anderson polyoxomolybdate anion. Supramolecular electrostatic coupling of the system to an iridium photosensitizer enables visible light-driven hydrogen evolution. Combined theory and experiment demonstrate the multifunctionality of the POM,

which acts as photosensitizer/catalyst-binding-site^[1] and facilitates light-induced charge-transfer and catalytic turnover. Chemical modification of the Pt-catalyst site leads to increased hydrogen evolution reactivity. Mechanistic studies shed light on the role of the individual components and provide a molecular understanding of the interactions which govern stability and reactivity. The system could serve as a blueprint for multifunctional polyoxometalates in energy conversion and storage.

Introduction

Supramolecular systems combine molecular-level control of structure and reactivity with the ability to deploy a range of specific intermolecular interactions to access new function. These concepts have led to groundbreaking developments ranging from supramolecular surface patterning^[2] to molecular machines^[3] and stimuli-responsive nanostructures.^[4] In the field of catalysis, supramolecular concepts have been developed to tune reactivity,^[1] selectivity as well as *in situ* catalyst assembly,^[5,6] highlighting the enormous potential of this field of research.

Over the last decade, pioneering studies have demonstrated the potential of supramolecular catalysis for energy conversion and storage,^[7,8] for example in the fields of water oxidation,^[9] CO₂ reduction,^[10] and the hydrogen evolution reaction

(HER).^[11,12] In light-driven HER catalysis, pioneering studies have demonstrated how supramolecular systems can be accessed by combining molecular catalysts with molecular photosensitizers. Often, component interactions are controlled by electrostatics, hydrogen bonding or π -stacking.^[13–15]

The design of molecular platforms is a central concept in supramolecular energy conversion, including HER, as it enables the merging of several functions in one molecule.^[16] So-called photochemical dyads utilize these concepts to combine photosensitizer, charge-transfer system and HER catalyst in one (supra)molecular assembly.^[17,18] One classical approach is the linkage of molecular photosensitizer (e.g. Ru-^[14,19,20] or Ir-complexes) and metal complex catalysts (e.g. Pt-^[21] Pd-^[22,23] Rh-^[14] or Co-based^[15,20]) using ditopic bridging ligands for charge-transfer.^[24] This has led to unique models, where insights into the photophysical and electronic properties as well as HER

[a] S. Maloul, A. K. Mengele, Prof. Dr. S. Rau, Prof. Dr. C. Streb
Institute of Inorganic Chemistry I
Ulm University
Albert-Einstein-Allee 11, 89081 Ulm (Germany)
E-mail: sven.rau@uni-ulm.de
carsten.streb@uni-ulm.de

[b] M. van den Borg, D. Gaissmaier, Prof. Dr. T. Jacob
Institute of Electrochemistry
Ulm University
Albert-Einstein-Allee 47, 89081 Ulm (Germany)
E-mail: timo.jacob@uni-ulm.de

[c] Dr. C. Müller, Prof. Dr. B. Dietzek-Ivanšić
Institute of Physical Chemistry
Friedrich Schiller University Jena
Helmholtzweg 4, 07743 Jena (Germany)
E-mail: benjamin.dietzek@uni-jena.de

[d] Dr. C. Müller, Dr. L. Zedler, Prof. Dr. B. Dietzek-Ivanšić
Leibniz Institute of Photonic Technologies (IPHT)
Albert-Einstein-Straße 9, 07745 Jena (Germany)

[e] D. Gaissmaier, Prof. Dr. T. Jacob
Helmholtz-Institute Ulm (HIU) Electrochemical Energy Storage
Helmholtzstr. 11, 89081 Ulm (Germany)

[f] D. Gaissmaier, Prof. Dr. T. Jacob
Karlsruhe Institute of Technology (KIT)
P.O. Box 3640, 76021 Karlsruhe (Germany)

[**] A previous version of this manuscript has been deposited on a preprint server (<https://doi.org/10.33774/chemrxiv-2021-d0fg9>).

Supporting information for this article is available on the WWW under <https://doi.org/10.1002/chem.202103817>

Part of a Special Issue on Contemporary Challenges in Catalysis.

© 2021 The Authors. Chemistry - A European Journal published by Wiley-VCH GmbH. This is an open access article under the terms of the Creative Commons Attribution License, which permits use, distribution and reproduction in any medium, provided the original work is properly cited.

activity have become possible using combined experiment and theory.^[14,19,24] This concept has been significantly expanded by recent studies where several photosensitizers were linked to HER catalytic sites, leading to operational supramolecular HER systems.^[25–27] Component optimization by chemical modification demonstrated the tunability of these systems, leading to in-depth understanding of function and reactivity limitations.^[14,21,23]

In recent years, the concept of supramolecular dyads has been expanded to the field of molecular metal oxides, or polyoxometalates (POMs). POMs are versatile dyad components, which can act as oxidation and reduction catalysts as well as charge separation^[28] and charge-storage sites.^[29,30] In addition, their structure and reactivity can be tuned over a wide range by chemical modification.^[31–35] This versatility has made POMs a research focus for advanced, light-driven energy conversion and storage.^[30,36–38] In particular, the covalent organo-functionalization of POMs has paved the way for the design of multifunctional platform molecules,^[39,40] where several functions can in principle be incorporated in one POM.^[32,33,41,42] This has led to ground-breaking studies in light-driven hydrogen evolution,^[27,43] photo-electrochemistry^[28] and nanocomposites for reversible electron storage.^[44] Building on these pioneering studies, we now report the use of POMs as multifunctional redox-active platform molecules capable of charge storage, HER catalyst anchoring as well as supramolecular photosensitizer binding.^[45] Using this approach, multiple functions can be combined in one molecular assembly, while independent reactivity tuning would be possible by modification of each component.

Here, we report a supramolecular approach to light-driven HER: an anionic Anderson-type platform-POM is covalently functionalized with a Pt(II)-complex HER catalyst. The compound is then electrostatically coupled in solution with a cationic iridium-photosensitizer (PS) to give the full supramolecular assembly. We demonstrate that in homogeneous solution, the system is capable of light-driven hydrogen evolution. Experimental and theoretical mechanistic studies show that the POM acts as PS- and catalyst-binding site, facilitating electron transfer under irradiation.

Results and Discussion

Catalyst synthesis and characterization

Briefly, the POM-platform molecules were synthesized in a one-pot reaction, where the 2,2'-bipyridine (bpy)-functionalized Anderson-anion precursor **POM-bpy** ($n\text{Bu}_4\text{N}$)₃[MnMo₆O₁₈{(OCH₂)₃CNCH(C₁₁H₉N₂)₂}]^[43] was reacted with the respective Pt-precursor ([Pt(DMSO)₂Cl₂]^[46] or [Pt(DMSO)₂]^[47] in water-free, de-aerated acetonitrile to give the POM-catalyst systems **POM-PtCl** ($n\text{Bu}_4\text{N}$)₃[MnMo₆O₁₈{(OCH₂)₃CNCH(C₁₁H₉N₂)PtCl₂}]₂ and **POM-PtI** ($n\text{Bu}_4\text{N}$)₃[MnMo₆O₁₈{(OCH₂)₃CNCH(C₁₁H₉N₂)PtI₂}]₂, see Supporting Information for synthetic and analytical details. The solid, orange products were re-dissolved in N,N-dimethyl formamide (DMF), and diffusion of EtOAc into the DMF solution gave orange crystals suitable for single-crystal X-

ray diffraction (scXRD). Yields: 70.2% (**POM-PtCl**), 76.4% (**POM-PtI**), yields based on Pt. **POM-PtCl** and **POM-PtI** were fully characterized by elemental analysis, NMR-, FTIR-spectroscopy and scXRD, see Supporting Information for details (CCDC reference numbers: 2099459 (**POM-PtCl**) and 2099460 (**POM-PtI**)). Note that when **POM-PtCl** and **POM-PtI** are discussed collectively, we will refer to them as **POM-PtX**.

Light-driven hydrogen evolution

The visible-light-driven HER activity of **POM-PtI** and **POM-PtCl** was examined using the photosensitizer [Ir(ppy)₂(bpy)]PF₆ (**PS**). **PS** was chosen due to its cationic charge, and the literature-known ability for light-driven electron transfer to POMs.^[27,48] In addition, (spectro-)electrochemical analyses of both **POM-PtX** species showed, that at least two electron transfers from the photoreduced **PS** ($E_{1/2}$ ca. -1.8 V vs. Fc^+/Fc)^[49] to **POM-PtX** is thermodynamically possible, as both **POM-PtX** systems feature two redox-processes at potentials more positive than -1.8 V (see Supporting Information, Table S2, Figures S3, S4).

Thus, light-driven catalytic studies were performed in water-free, de-aerated DMF solutions containing the respective catalyst **POM-PtX** (12.5 μM), the photosensitizer **PS** (125 μM) and triethyl amine/acetic acid (TEA (1.0 M)/HAc (0.2 M)) as sacrificial proton/electron donors; this experimental setup has been adapted from earlier POM-based HER studies.^[48,50–52] The samples were irradiated under an Ar atmosphere using monochromatic LEDs ($\lambda_{\text{max}} = 470$ nm, $P \sim 40$ mW cm⁻²) at 25 °C. Hydrogen evolution was quantified by calibrated gas chromatography. Each data-point was recorded in triplicate, and averaged turnover numbers (*TONs*) are given based on the molar amount of Pt present, i.e., $\text{TON} = n(\text{H}_2)/n(\text{Pt})$. The non-modified catalysts [Pt(bpy)Cl₂]/[Pt(bpy)I₂] (25 μM) together with **PS** (125 μM) were used as references. Also, control experiments without irradiation or in the absence of POM-catalysts show virtually no H₂ evolution (Supporting Information, Figure S5).

First, the HER activity of **POM-PtCl** and the reference [Pt(bpy)Cl₂] were studied. It was observed that under irradiation H₂ evolution increases linearly with time for both catalysts, see Figure 2. After $t_{\text{irradiation}} = 10$ h, notable reactivity differences are observed. For **POM-PtCl** the *TONs* reached ~ 540 , while the reference [Pt(bpy)Cl₂] only exhibits a *TON* of ca. 400.

To further enhance the activity of the catalyst, the chloride ions on the Pt centers were replaced with iodide to give the **POM-PtI** cluster (see synthetic discussion above for details). When employed for light-driven HER under identical conditions as described above, **POM-PtI** showed significantly higher activity with a maximum *TON* of ca. 740 after $t_{\text{irradiation}} = 10$ h (Figure 2). Note that the higher reactivity of **POM-PtI** compared with **POM-PtCl** is in line with previous reports: for the related compounds ([Ru(tbbpy)₂(tpphz)PtX₂](PF₆)₂ (X = Cl or I), a similar increase of HER activity is found when the chloride ligands are replaced by iodides.^[21] The authors assigned this increased activity to the higher electron density at the Pt center due to the large, easily polarized iodide ligands.^[21] To the best of our

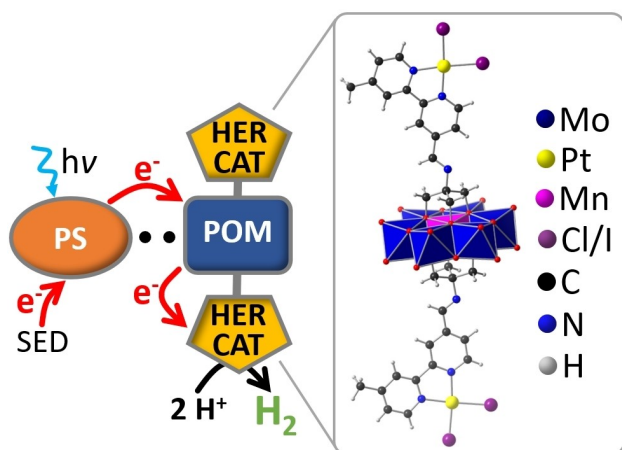


Figure 1. Left: Schematic illustration of the supramolecular photochemical system for visible light-driven hydrogen evolution. An anionic POM-platform molecule is covalently functionalized with a molecular Pt-HER catalyst. The system is electrostatically coupled to a cationic photosensitizer (PS). SED – sacrificial electron-donor. Right: molecular structure of the POM-PtX-platform (X = Cl, I, shown here: X = I, for crystallographic data see Supporting Information).

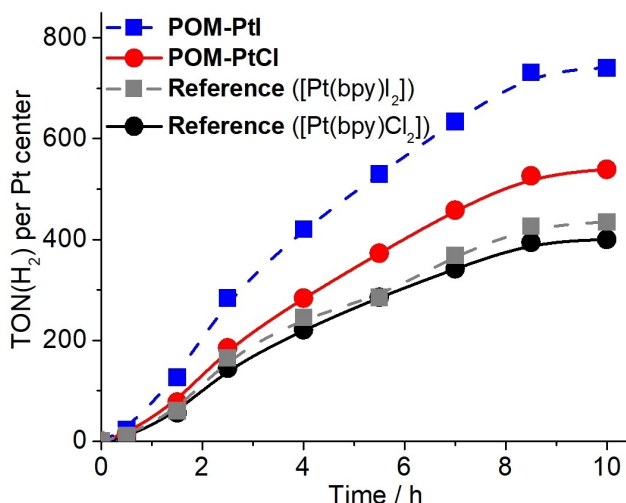


Figure 2. Light-driven HER activity of POM-PtCl (red), POM-PtI (blue) and the reference compounds [Pt(bpy)Cl₂] (black) and [Pt(bpy)I₂] (gray), showing the hydrogen evolution TON (calculated per Pt center) over time. Conditions: solvent: water-free, de-gassed DMF containing TEA (1.0 M) and HAc (0.2 M). c(POM-PtX) = 12.5 μM; c([Pt(bpy)X₂]) = 25 μM, c(PS) = 125 μM, irradiation: LED, λ_{max} = 470 nm, P ~ 40 mW cm⁻².

knowledge, this is the first time that ligand-tuning concepts have been demonstrated in POM-based HER catalysis.

Based on the above data, we propose that the increased activity of POM-PtCl and POM-PtI compared to the references is due to enhanced electrostatic attraction between the cationic PS and the anionic POM-catalyst. This could enable aggregation and charge-transfer in solution. To test this hypothesis, we performed a combined experimental and theoretical study which explores the interactions between PS and POM-PtX. Due to the higher reactivity, the study used POM-PtI as model.

Mechanistic photophysical studies

To assess the supramolecular interactions between photosensitizer and catalyst, we examined the emission quenching of PS by the electron acceptor POM-PtI or the sacrificial electron donor TEA (Figure 3a–d).^[53] The steady-state emission spectra and emission lifetimes of PS (λ_{excitation} = 420 nm) were measured upon addition of TEA or POM-PtI to a DMF solution of PS (see Figure 3a,c and Supporting Information, Figure S7). The corresponding Stern-Volmer plots (Figure 3b,d and Supporting Information, Figures S7, S8) are analyzed by linear fitting resulting in quenching rate constants (k_q) of 7.1 × 10⁷ M⁻¹s⁻¹ (reductive quenching, TEA) and 8.4 × 10¹⁰ M⁻¹s⁻¹ (oxidative quenching, POM-PtI). The calculated mutual diffusion rate constants (k_D) in DMF are 7.7 × 10⁹ M⁻¹s⁻¹ (for PS/TEA) and 8.2 × 10⁹ M⁻¹s⁻¹ (for PS/POM-PtI), respectively (see Supporting Information, Section 7). Comparison between k_D and k_q however shows that for reductive quenching (PS*/TEA) k_D is ~100 times higher than k_q, indicating a quenching efficiency per encounter of ca. 1%.^[54] In contrast, for the oxidative quenching (PS*/POM-PtI) k_D is ~10 times smaller than k_q, indicating a quenching efficiency per encounter of formally >100%. Two interpretations are in line with these observations: (a) the interactions of the PS cation and the POM-PtI anion increase the rate of interaction beyond the frequency calculated for neutral reaction partners within the Collins-Kimball model (see Supporting Information, Section 7);^[55] (b) a supramolecular pre-assembly of cationic PS and anionic POM-PtI enables PS* quenching at significantly faster rates than the mutual diffusion, i.e., in the limit of static quenching.^[56] As a result, the oxidative quenching of PS* has to occur via both, static and dynamic quenching.

Next, the quenching efficiency of PS by the anionic POM-PtI was compared with the quenching behavior of the charge-neutral [Pt(bpy)I₂] reference (Figure 3e). Here, POM-PtI showed a significantly higher quenching efficiency compared to the reference compound. This supports the suggestion that electrostatic attraction of PS and POM-PtI in solution can be used to enhance electronic interactions of the reaction partners following photoexcitation of the PS. This observation also supports the HER catalytic findings, where POM-PtI shows significantly higher reactivity than the [Pt(bpy)I₂] reference (Figure 2).

Theoretical studies of PS/POM-PtI aggregation

To better understand the coupling between PS and POM-PtCl and its effects on the electronic properties of the system, first principles simulations using spin-polarized density functional theory (DFT) calculations within the ORCA program package were performed.^[57] Initial geometry optimization used the PBEh-3c composite method^[58] followed by geometry optimizations with the PBE0 hybrid functional^[59,60] and a def2-TZVP basis set.^[61] For molybdenum and iridium, effective core potentials were used to replace the core electrons.^[62,63] Dispersion interactions were accounted for by atom-pairwise correction with the Becke–Johnson damping scheme [D3(BJ)].^[64,65] The conductor-like polarizable continuum model (CPCM) was used

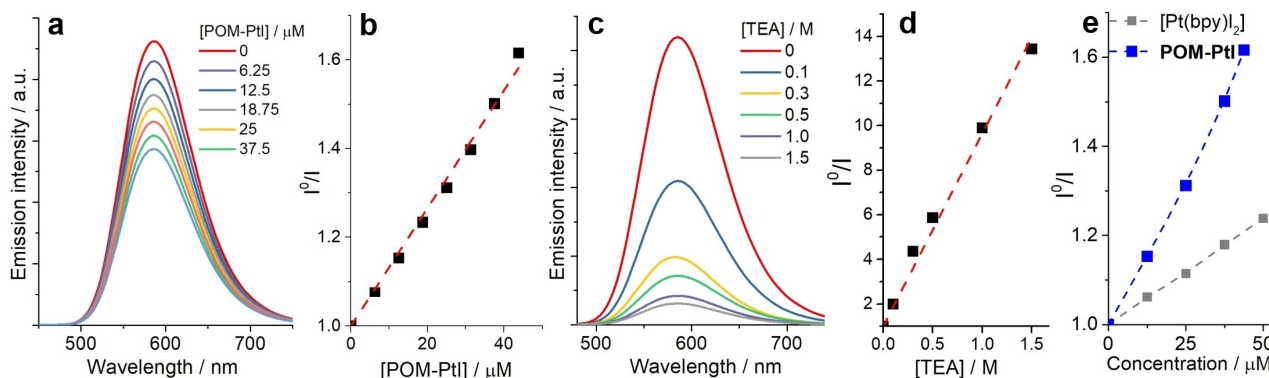


Figure 3. (a) Emission quenching spectra of PS ($[\text{Ir}(\text{ppy})_2(\text{bpy})]^+$, 125 μM) as a function of [POM-PtI], and (b) corresponding Stern-Volmer plot; (c) emission quenching spectra of PS ($[\text{Ir}(\text{ppy})_2(\text{bpy})]^+$, 125 μM) as a function of [TEA], and (d) corresponding Stern-Volmer plot; (e) Stern-Volmer plot, comparing the emission quenching of PS by POM-PtI and the $[\text{Pt}(\text{bpy})_2]$ reference. Conditions: water-free, de-aerated DMF, details see Supporting Information, Section 7.

to implicitly include the DMF solvent ($\epsilon = 38.30$ and $n = 1.43$).^[66] Electron densities were analyzed by Hirshfeld population analysis to determine atomic charges.^[67]

To gain insights into the energetics and binding behavior of PS and POM-PtX, we used DFT calculations to assess the interaction energies between both species. As model systems, we focused on PS (charge: 1+) and POM-PtCl (charge: 3-), see Figure 4. As references, we studied $[\text{Pt}(\text{bpy})\text{Cl}_2]$ (charge-neutral) and the TRIS-functionalized prototype Anderson anion $[\text{MnMo}_6\text{O}_{18}\{(\text{CH}_2\text{O})_3\text{CNH}_2\}_2]^{3-}$ (POM-Ref, charge: 3-, Supporting Information, Figure S9).^[43] Initial studies gave interaction ener-

gies of -48 kJ/mol (PS/ $[\text{Pt}(\text{bpy})\text{Cl}_2]$) and -76 kJ/mol (PS/POM-Ref) and -77 kJ/mol (PS/POM-PtCl), respectively. This highlights, that supramolecular aggregation in solution between photosensitizer and POM is thermodynamically favored. For the PS/POM-PtCl system, we observe that in the energetically most favored system, PS is located next to the metal oxo cluster (Figure 4), highlighting the importance of the POM for PS-binding. Note that quantitatively virtually identical results were obtained for POM-PtI; these are shown in the Supporting Information, Section 8).

Next, we theoretically assessed the electronic consequences of an electron-transfer from PS to POM-PtCl, which is a key redox step of the HER catalytic cycle. To this end, single-point calculations were performed on the one-electron reduced POM-PtCl as well as the one-electron reduced reference systems (i.e., $[\text{Pt}(\text{bpy})\text{Cl}_2]$ and POM-Ref). This allowed us to compare the Hirshfeld net charges of the one-electron reduced systems with the charge-distribution of the non-reduced systems. Note that this procedure is analogous to determining condensed Fukui functions.^[68,69] While Fukui functions are often used as descriptors for the chemical reactivity of a molecule (with respect to its electrophilic and nucleophilic regions), here, the function for a nucleophilic attack will serve as a measure for the uptake and distribution of additional electron density in the systems studied. The Fukui function f^+ is given by the difference between the electron densities of the initial state $\rho(N)$ and the state featuring one additional electron $\rho(N+1)$:

$$f^+ = \rho(N+1) - \rho(N)$$

The corresponding condensed Fukui function f_k^+ is defined as:

$$f_k^+ = q_k(N+1) - q_k(N)$$

where $q_k(N)$ describes the atomic charges at the respective atomic center k of the original system and $q_k(N+1)$ those of the system with one additional electron. After normalization, this provides a percentage value of the additional electron

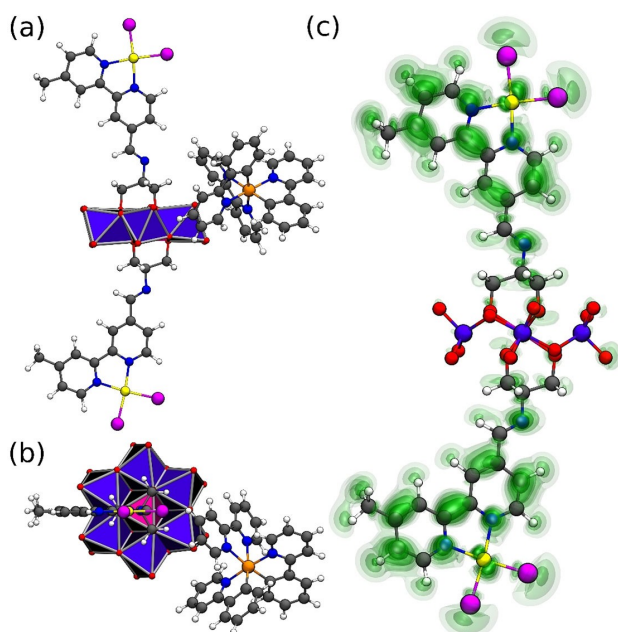


Figure 4. Energetically most favored interaction sites between PS and POM-PtI in (a) side view and (b) top view; (c) representation of the f^+ Fukui function calculated for the one-electron reduced POM-PtCl, shown as charge-difference plot. The iso-surfaces correspond to electron-accepting regions where an additional added electron will be located (as indicated by the f^+ Fukui function). Regions with higher values are marked in darker shades of green. Molecular color scheme, see Figure 1.

density at any given atom. For clarity, we have combined the resulting atomic percentages into three molecular sub-units, i.e. the 2,2'-bipyridine ligands (bpy), the platinum-chloride fragment $\{PtCl_2\}$ and the POM metal-oxo framework $\{MnMo_6O_{24}\}$, see Table 1 and Supporting Information, Section 8 for computational details.

As shown in Table 1, analysis of the nucleophilic Fukui function for the one-electron reduced POM-PtCl indicates that additional electron density will be distributed on the Pt-HER catalyst, either on the $\{PtCl_2\}$ fragment (18.8%) or the bpy ligand (75.5%), while only a low percentage of the additional electron is distributed on the POM framework (5.7%). For the reference systems, the expected distributions are observed: in POM-Ref, 88.6% of the electron density is located on the POM framework, while in $[Pt(bpy)Cl_2]$, 79.7% are located on the bpy and 20.3% on the $\{PtCl_2\}$ fragment (Figure 4 and Supporting Information, Table S3). This is in line with experimental electrochemical and spectro-electrochemical data, which indicate that an electron transfer to the one-electron reduced POM-PtX, i.e., a second reduction of POM-PtX occurs on the $\{Pt(bpy)X_2\}$ moiety (Supporting Information, Figures S3, S4).

Reusability and stability of the molecular catalyst: Finally, we were interested in understanding the causes of the loss of HER activity observed after ~ 9 h of irradiation (Figure 2). We hypothesized (based on initial UV-Vis spectroscopy of the reaction solution, Supporting Information, Figure S10), that this could be due to PS degradation, and thus, loss of the light-harvesting capabilities of the system. In contrast, prolonged visible light-irradiation of POM-PtX resulted in minor UV-Vis absorption changes in the 400–450 nm region. This could indicate a very slow degradation (Supporting Information, Figure S11), which is currently being studied by *in situ* optical and vibrational spectroscopies. To experimentally demonstrate that PS degradation is the main deactivation pathway under the given conditions, we performed a reusability experiment where the standard photochemical experiment (identical to the experiment shown in Figure 2, catalyst: POM-PtI) was performed. After 10 h of irradiation, an aliquot of fresh PS (110 μ M) was added to the reaction mixture and irradiation was resumed. As illustrated in Figure 5, the system resumed hydrogen evolution at high reactivity. This observation provides evidence that PS degradation is a major factor in reactivity loss in the system described, while catalytic activity by the POM-PtI is still observed. Thus, future studies can explore the design of more robust photosensitizers with optimized POM binding behavior.^[70]

To gain further insight into the stability of POM-PtX, we performed a range of mechanistic analyses: First, UV-Vis

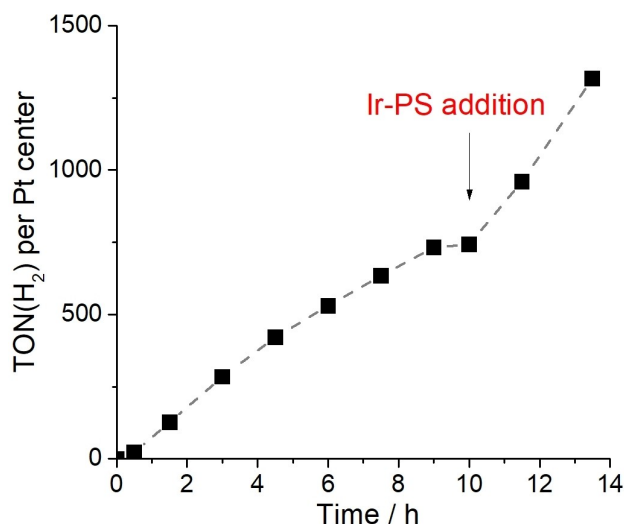


Figure 5. Reusability of the catalyst POM-PtI demonstrated by adding an aliquot of PS after HER activity ceased (after $t_{\text{irradiation}} = 10$ h). Conditions are identical to the HER experiments shown in Figure 2

spectroscopy of POM-PtX in the reaction solvent DMF showed no spectral changes over 18 h (Supporting Information, Figure S11). Also, microfiltration and UV-Vis spectroscopic analysis of a reaction mixture containing POM-PtI and PS (molar ratio: 1/10) showed no spectral changes, indicating that no colloidal particles are observed (Supporting Information, Figure S12). This was supported by dynamic light scattering (DLS) on the catalytic reaction solution, where no particles within the measurement range (1–10000 nm) were detected. This suggests that the system does not produce colloidal platinum particles as the active HER catalyst, but that a molecular system operates as HER catalyst in the present study. Note that the “classical” mercury amalgam test for Pt colloids was not suitable for the present system, as elemental Hg undergoes redox-reactions with POM-PtX already in the dark, resulting in fast degradation of the POM-PtX molecule. Similar behavior has been reported before.^[21]

To provide further evidence for the molecular nature of the HER system reported, we performed a catalytic experiment under the standard conditions described in Figure 2 using POM-PtCl as model catalyst. Then, excess nBu_4NI was added to the reaction solution to trigger iodide-for chloride ligand exchange on POM-PtCl (leading to partial *in situ* formation of POM-PtI). As predicted from our initial experiments (Figure 2), this led to an increase of the TON (+ $\sim 20\%$), thereby providing further evidence of a molecular HER catalysis (Supporting Information, Figure S13).^[71,72]

Conclusion

In sum, we demonstrate how organo-functionalized polyoxo-metalates can be used as multifunctional platforms for supramolecular light-driven hydrogen evolution catalysis. Electrostatic solution-interactions between an anionic, Pt-function-

Table 1. Percentage distribution of an additional electron taken up by POM-PtCl, POM-Ref and $[Pt(bpy)Cl_2]$ as calculated using normalized nucleophilic Fukui functions f_k^+ and Hirshfeld population analysis.

Fragment	POM-PtCl	POM-Ref	$[Pt(bpy)Cl_2]$
bpy	75.5	–	79.7
$\{PtCl_2\}$	18.8	–	20.3
$\{MnMo_6O_{24}\}$	5.7	88.6	–

alized POM dyad with a cationic photosensitizer lead to light-driven charge-transfer and H₂ evolution in solution. The reactivity of the dyads surpasses the purely intermolecular reference systems, and reactivity tuning of the dyads is possible by ligand exchange. Experiment and theory shed light on the underlying interactions in solution, and initial stability analyses highlight future areas of development, such as the shift from organic to aqueous solvents. Our results open new avenues for the design of supramolecular light-driven hydrogen evolution catalysts.

Experimental Section

Deposition Numbers 2099459 (for POM-PtCl) and 2099460 (for POM-PtI) contain the supplementary crystallographic data for this paper. These data are provided free of charge by the joint Cambridge Crystallographic Data Centre and Fachinformationszentrum Karlsruhe Access Structures service.

Acknowledgements

Financial support by the Deutsche Forschungsgemeinschaft DFG through the Transregio-Collaborative Research Center TRR234 CATALIGHT, project no 364549901, projects A1, A4 and A5 and the priority program SPP2102 *Light-controlled reactivity of metal complexes*, project no 359737763 is gratefully acknowledged. C.M. gratefully acknowledges support by the Fonds der Chemischen Industrie FCI through a Kekulé fellowship. S.M. gratefully acknowledges financial support by the Deutscher Akademischer Austauschdienst DAAD and the Schlumberger Foundation (Faculty for the future program). We gratefully acknowledge Ilse E. Friedländer for assistance with spectro-electrochemical measurements. Open Access funding enabled and organized by Projekt DEAL.

Conflict of Interest

The authors declare no conflict of interest.

Data Availability Statement

The data that support the findings of this study are available from the corresponding author upon reasonable request.

Keywords: hydrogen evolution · organic-inorganic hybrid · polyoxometalate · self-assembly · supramolecular

- [1] S. Karlsson, J. Boixel, Y. Pellegrin, E. Blart, H.-C. Becker, F. Odobel, L. Hammarström, *Faraday Discuss.* **2012**, *155*, 233–252.
- [2] D. P. Goronzy, M. Ebrahimi, F. Rosei, Arramel, Y. Fang, S. De Feyter, S. L. Tait, C. Wang, P. H. Beton, A. T. S. Wee, et al., *ACS Nano* **2018**, *12*, 7445–7481.
- [3] R. Iino, K. Kinbara, Z. (guest eds) Bryant, *Chem. Rev.* **2020**, *120*, 1–460.
- [4] Z. Li, N. Song, Y.-W. Yang, *Matter* **2019**, *1*, 345–368.
- [5] J. Meeuwissen, J. N. H. Reek, *Nat. Chem.* **2010**, *2*, 615–621.

- [6] M. Raynal, P. Ballester, A. Vidal-Ferran, P. W. N. M. van Leeuwen, *Chem. Soc. Rev.* **2014**, *43*, 1660–1733.
- [7] B. Zhang, L. Sun, *Chem. Soc. Rev.* **2019**, *48*, 2216–2264.
- [8] T. Keijer, T. Bouwens, J. Hessels, J. N. H. Reek, *Chem. Sci.* **2021**, *12*, 50–70.
- [9] V. Kunz, D. Schmidt, M. I. S. Röhr, R. Mitrić, F. Würthner, *Adv. Energy Mater.* **2017**, *7*, 1602939.
- [10] Y. Tamaki, O. Ishitani, *ACS Catal.* **2017**, *7*, 3394–3409.
- [11] F. Gärtner, B. Sundararaju, A. E. Surkus, A. Boddien, B. Loges, H. Junge, P. H. Dixneuf, M. Beller, *Angew. Chem. Int. Ed.* **2009**, *48*, 9962–9965; *Angew. Chem.* **2009**, *121*, 10147–10150.
- [12] A. Neubauer, G. Grell, A. Friedrich, S. I. Bokarev, P. Schwarzbach, F. Gärtner, A.-E. Surkus, H. Junge, M. Beller, O. Kühn, et al., *J. Phys. Chem. Lett.* **2014**, *5*, 1355–1360.
- [13] D. R. Whang, S. Y. Park, *ChemSusChem* **2015**, *8*, 3204–3207.
- [14] T. A. White, B. N. Whitaker, K. J. Brewer, *J. Am. Chem. Soc.* **2011**, *133*, 15332–15334.
- [15] J. Dong, M. Wang, P. Zhang, S. Yang, J. Liu, X. Li, L. Sun, *J. Phys. Chem. C* **2011**, *115*, 15089–15096.
- [16] J. J. Walsh, A. M. Bond, R. J. Forster, T. E. Keyes, *Coord. Chem. Rev.* **2016**, *306*, 217–234.
- [17] V. Balzani, A. Credi, M. Venturi, *ChemSusChem* **2008**, *1*, 26–58.
- [18] F. Odobel, M. Séverac, Y. Pellegrin, E. Blart, C. Fosse, C. Cannizzo, C. R. Mayer, K. J. Elliott, A. Harriman, *Chem. Eur. J.* **2009**, *15*, 3130–3138.
- [19] S. Tschierlei, M. Karnahl, M. Presselt, B. Dietzek, J. Guthmüller, L. González, M. Schmitt, S. Rau, J. Popp, *Angew. Chem. Int. Ed.* **2010**, *49*, 3981–3984; *Angew. Chem.* **2010**, *122*, 4073–4076.
- [20] A. Fihri, V. Artero, M. Razavet, C. Baffert, W. Leibl, M. Fontecave, *Angew. Chem. Int. Ed.* **2008**, *47*, 564–567; *Angew. Chem.* **2008**, *120*, 574–577.
- [21] M. G. Pfeffer, T. Kowacs, M. Wächtler, J. Guthmüller, B. Dietzek, J. G. Vos, S. Rau, *Angew. Chem. Int. Ed.* **2015**, *54*, 6627–6631; *Angew. Chem.* **2015**, *127*, 6727–6731.
- [22] S. Rau, B. Schäfer, D. Gleich, E. Anders, M. Rudolph, M. Friedrich, H. Görls, W. Henry, J. G. Vos, *Angew. Chem. Int. Ed.* **2006**, *45*, 6215–6218; *Angew. Chem.* **2006**, *118*, 6361–6364.
- [23] M. G. Pfeffer, B. Schäfer, G. Smolentsev, J. Uhlig, E. Nazarenko, J. Guthmüller, C. Kuhnt, M. Wächtler, B. Dietzek, V. Sundström, S. Rau, *Angew. Chem. Int. Ed.* **2015**, *54*, 5044–5048; *Angew. Chem.* **2015**, *127*, 5132–5136.
- [24] M. Schulz, M. Karnahl, M. Schwalbe, J. G. Vos, *Coord. Chem. Rev.* **2012**, *256*, 1682–1705.
- [25] M. Elvington, J. Brown, S. M. Arachchige, K. J. Brewer, *J. Am. Chem. Soc.* **2007**, *129*, 10644–10645.
- [26] S. Chen, K. Li, F. Zhao, L. Zhang, M. Pan, Y.-Z. Fan, J. Guo, J. Shi, C.-Y. Su, *Nat. Commun.* **2016**, *7*, 13169.
- [27] B. Matt, J. Fize, J. Moussa, H. Amouri, A. Pereira, V. Artero, G. Izzet, A. Proust, *Energy Environ. Sci.* **2013**, *6*, 1504–1508.
- [28] F. A. Black, A. Jacquart, G. Toupalas, S. Alves, A. Proust, I. P. Clark, E. A. Gibson, G. Izzet, *Chem. Sci.* **2018**, *9*, 5578–5584.
- [29] B. Rausch, M. D. Symes, G. Chisholm, L. Cronin, *Sci. J.* **2014**, *345*, 1326–1330.
- [30] L. G. Bloor, R. Solarska, K. Bienkowski, P. J. Kulesza, J. Augustynski, M. D. Symes, L. Cronin, *J. Am. Chem. Soc.* **2016**, *138*, 6707–6710.
- [31] Special POM-themed issue, L. Cronin, A. Müller (guest eds.), *Chem. Soc. Rev.* **2012**, *41*, 7325–7648.
- [32] A. V. Anyushin, A. Kondinski, T. N. Parac-Vogt, *Chem. Soc. Rev.* **2020**, *49*, 382–432.
- [33] A. Proust, B. Matt, R. Villanneau, G. Guillemot, P. Gouzerh, G. Izzet, *Chem. Soc. Rev.* **2012**, *41*, 7605–7622.
- [34] K. J. Elliott, A. Harriman, L. Le Pleux, Y. Pellegrin, E. Blart, C. R. Mayer, F. Odobel, *Phys. Chem. Chem. Phys.* **2009**, *11*, 8767–8773.
- [35] A. Harriman, K. J. Elliott, M. a. H. Alamiry, L. Le Pleux, M. Séverac, Y. Pellegrin, E. Blart, C. Fosse, C. Cannizzo, C. R. Mayer, et al., *J. Phys. Chem. C* **2009**, *113*, 5834–5842.
- [36] C. Streb, *Dalton Trans.* **2012**, *41*, 1651.
- [37] H. Lv, Y. V. Geletii, C. Zhao, J. W. Vickers, G. Zhu, Z. Luo, J. Song, T. Lian, D. G. Musaev, C. L. Hill, *Chem. Soc. Rev.* **2012**, *41*, 7572–7589.
- [38] A. Sartorel, M. Carraro, F. M. Toma, M. Prato, M. Bonchio, *Energy Environ. Sci.* **2012**, *5*, 5592–5603.
- [39] Y.-F. Song, R. Tsunashima, *Chem. Soc. Rev.* **2012**, *41*, 7384.
- [40] G. Izzet, F. Volatron, A. Proust, *Chem. Rec.* **2017**, *17*, 250–266.
- [41] A. J. Kibler, G. N. Newton, *Polyhedron* **2018**, *154*, 1–20.
- [42] A. Blazevic, A. Rompel, *Coord. Chem. Rev.* **2016**, *307*, Part, 42–64.
- [43] S. Schönweiz, S. A. Rommel, J. Kübel, M. Mischeel, B. Dietzek, S. Rau, C. Streb, *Chem. Eur. J.* **2016**, *22*, 12002–12005.

- [44] E. Hampson, J. M. Cameron, S. Amin, J. Kyo, J. A. Watts, H. Oshio, G. N. Newton, *Angew. Chem. Int. Ed.* **2019**, *58*, 18281–18285; *Angew. Chem.* **2019**, *132*, 14437–14441.
- [45] M. Bonchio, Z. Syrgiannis, M. Burian, N. Marino, E. Pizzolato, K. Dirian, F. Rigodanza, G. A. Volpato, G. La Ganga, N. Demitri, et al., *Nat. Chem.* **2019**, *11*, 146–153.
- [46] T. A. K. Al-Allaf, L. J. Rashan, A. S. Abu-Surrah, R. Fawzi, M. Steimann, *Transition Met. Chem.* **1998**, *23*, 403–406.
- [47] T. Kowacs, L. O'Reilly, Q. Pan, A. Huijser, P. Lang, S. Rau, W. R. Browne, M. T. Pryce, J. G. Vos, *Inorg. Chem.* **2016**, *55*, 2685–2690.
- [48] Y. Luo, S. Maloul, M. Wächtler, A. Winter, U. S. Schubert, C. Streb, B. Dietzek, *Chem. Commun.* **2020**, *56*, 10485–10488.
- [49] Y. Ohsawa, S. Sprouse, K. A. King, M. K. DeArmond, K. W. Hanck, R. J. Watts, *J. Phys. Chem.* **1987**, *91*, 1047–1054.
- [50] S. Schönweiz, M. Heiland, M. Anjass, T. Jacob, S. Rau, C. Streb, *Chem. Eur. J.* **2017**, *23*, 15370–15376.
- [51] S. Schönweiz, S. Knoll, M. Anjass, M. Braumüller, S. Rau, C. Streb, n.d.
- [52] Y. Luo, S. Maloul, S. Schönweiz, M. Wächtler, C. Streb, B. Dietzek, *Chem. A Eur. J.* **2020**, *26*, 8045–8052.
- [53] B. M. Hockin, C. Li, N. Robertson, E. Zysman-Colman, *Catal. Sci. Technol.* **2019**, *9*, 889–915.
- [54] A. Neubauer, G. Grell, A. Friedrich, S. I. Bokarev, P. Schwarzbach, F. Gärtner, A.-E. Surkus, H. Junge, M. Beller, O. Kühn, et al., *J. Phys. Chem. Lett.* **2014**, *5*, 1355–1360.
- [55] F. C. Collins, G. E. Kimball, *J. Colloid Sci.* **1949**, *4*, 425–437.
- [56] L. M. Kiefer, K. J. Kubarych, *Chem. Sci.* **2018**, *9*, 1527–1533.
- [57] F. Neese, *Wiley Interdiscip. Rev.: Comput. Mol. Sci.* **2018**, *8*, e1327.
- [58] S. Grimme, J. G. Brandenburg, C. Bannwarth, A. Hansen, *J. Chem. Phys.* **2015**, *143*, 054107.
- [59] J. P. Perdew, M. Ernzerhof, K. Burke, *J. Chem. Phys.* **1996**, *105*, 9982–9985.
- [60] C. Adamo, V. Barone, *J. Chem. Phys.* **1999**, *110*, 6158–6170.
- [61] F. Weigend, R. Ahlrichs, *Phys. Chem. Chem. Phys.* **2005**, *7*, 3297.
- [62] K. Eichkorn, F. Weigend, O. Treutler, R. Ahlrichs, *Theor. Chem. Accounts Theory, Comput. Model. (Theoretica Chim. Acta)* **1997**, *97*, 119–124.
- [63] D. Andrae, U. Häußermann, M. Dolg, H. Stoll, H. Preuß, *Theor. Chim. Acta* **1991**, *78*, 247–266.
- [64] S. Grimme, J. Antony, S. Ehrlich, H. Krieg, *J. Chem. Phys.* **2010**, *132*, 154104.
- [65] S. Grimme, S. Ehrlich, L. Goerigk, *J. Comput. Chem.* **2011**, *32*, 1456–1465.
- [66] M. Cossi, N. Rega, G. Scalmani, V. Barone, *J. Comput. Chem.* **2003**, *24*, 669–681.
- [67] F. L. Hirshfeld, *Theor. Chim. Acta* **1977**, *44*, 129–138.
- [68] K. Fukui, T. Yonezawa, H. Shingu, *J. Chem. Phys.* **1952**, *20*, 722–725.
- [69] R. G. Parr, W. Yang, *J. Am. Chem. Soc.* **1984**, *106*, 4049–4050.
- [70] K. Heussner, K. Peuntinger, N. Rockstroh, L. C. Nye, I. Ivanovic-Burmazovic, S. Rau, C. Streb, *Chem. Commun. (Camb.)* **2011**, *47*, 6852–6854.
- [71] S. A. De Pascali, D. Migoni, P. Papadia, A. Muscella, S. Marsigliante, A. Ciccacese, F. P. Fanizzi, *Dalton Trans.* **2006**, *2*, 5077–5087.
- [72] M. González, R. Bartolomé, S. Matarraz, E. Rodríguez-Fernández, J. L. Manzano, M. Pérez-Andrés, A. Orfao, M. Fuentes, J. J. Criado, *J. Inorg. Biochem.* **2012**, *106*, 43–45.

Manuscript received: October 22, 2021

Accepted manuscript online: October 31, 2021

Version of record online: November 11, 2021